

INFLUENCE OF ADAS ELEMENT PARAMETERS ON BUILDING SEISMIC RESPONSE

By Chuan Xia,¹ Associate Member, ASCE, and Robert D. Hanson,² Member, ASCE

ABSTRACT: Supplemental damping devices have been used to decrease the dynamic response of buildings subjected to wind and earthquake inputs. These devices can be generalized into the following three major types: friction devices, viscous or viscoelastic devices, and material yield devices. Lead dampers would be included in this last case, even though its characteristics do not involve yielding. A study of one of the metallic yield devices, the steel-plate added damping and stiffness (ADAS) device, is presented. Yield force, yield displacement, strain-hardening ratio, ratio of the device stiffness to the bracing member stiffness, and ratio of device stiffness to structural story stiffness without the device in place have been identified as the most important parameters to characterize the performance of this device. The influence of these parameters on earthquake response of building structures is analyzed. The results show that these devices can substantially increase the energy dissipation capacity of a structure and significantly reduce the energy dissipation demand on the framing members of a structure.

INTRODUCTION

A number of imaginative approaches to improved earthquake response performance and damage control have been developed and others will be forthcoming. These can be divided into two groups, passive systems, of which base isolation and supplemental mechanical damping are examples, and active systems, which require active participation of mechanical devices whose inputs depend upon measured building response. The subject of this paper deals only with one member of a family of passive supplemental mechanical damping systems. It will be shown that these supplemental damping systems can provide performance advantages for the earthquake design of new buildings and retrofit upgrading of the seismic resistance of existing buildings. This paper focuses on one of several supplemental damping systems, but its results could be applicable to others.

The steel-plate added damping and stiffness (ADAS) device is an assemblage of steel plates that is designed for installation in a building frame such that the relative story drift causes the top of the device to move horizontally relative to the bottom, as shown in Figs. 1 and 2. By yielding a large volume of steel, the ADAS device can dissipate substantial energy during an earthquake.

There are a number of benefits of dissipating energy through the yielding of ADAS devices: (1) Energy dissipation is concentrated at locations that have been designed for this purpose; (2) energy dissipation demands on other structural members can be substantially reduced; and (3) yielding of the ADAS devices will not affect the gravity load service capacity of the structural system, because the devices are part of the lateral load resisting

¹Engr., The Austin Co., 800 S.W. 16th St., Renton, WA 98055.

²Prof., Dept. of Civ. Engrg., Univ. of Michigan, Ann Arbor, MI 48109-2125.

Note. Discussion open until December 1, 1992. To extend the closing date one month, a written request must be filed with the ASCE Manager of Journals. The manuscript for this paper was submitted for review and possible publication on April 29, 1991. This paper is part of the *Journal of Structural Engineering*, Vol. 118, No. 7, July, 1992. ©ASCE, ISSN 0733-9445/92/0007-1903/\$1.00 + \$.15 per page. Paper No. 1762.

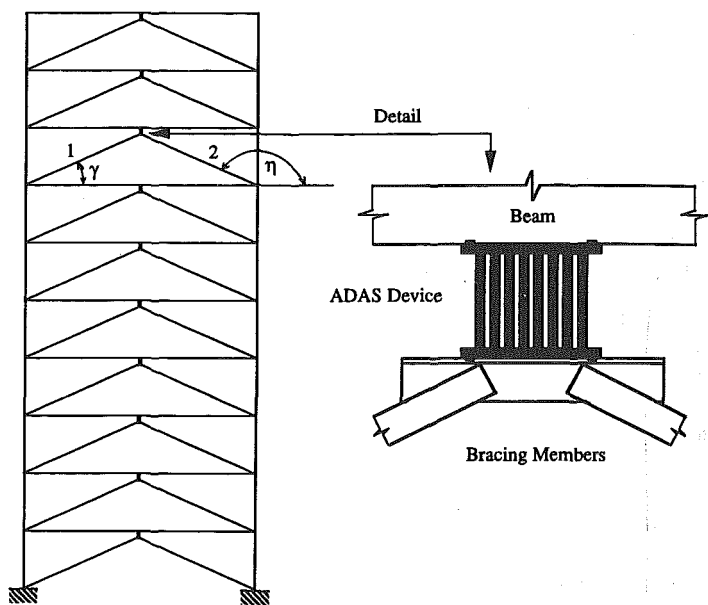


FIG. 1. Frames with ADAS Devices and V-Shaped Bracing Members

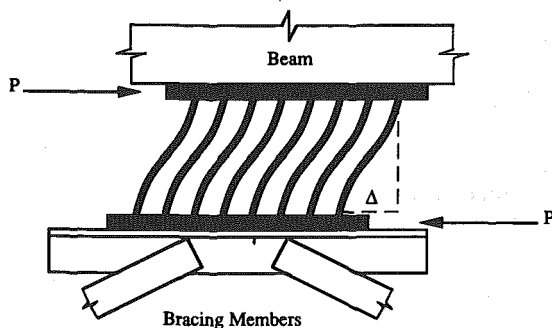


FIG. 2. Force and Displacement of ADAS Devices

system only. The ADAS devices can be easily replaced after an earthquake, if necessary.

The mechanical characteristics of yielding steel devices were investigated by a number of researchers (Steimer and Chow 1984; Scholl 1990; Hanson 1986; Bergman and Hanson 1986, 1990; Whittaker et al. 1989; Su and Hanson 1990a, 1990b). The tests of ADAS devices and frames with ADAS elements showed that the ADAS devices are very reliable energy dissipators that exhibit stable hysteretic behavior for displacement amplitudes as large as 14 times the device yield displacement, Δ_y , and are well suited for use in building structures situated in high seismic risk zones (Whittaker et al. 1989). The tests at the University of California at Berkeley found that in the displacement range of $6 \Delta_y$ or less, the ADAS device hysteretic behavior is dependent only on the yield force, P_y , and the yield displacement, Δ_y ,

and can sustain an extremely large number of yielding reversals (more than 100 cycles in the tests). A bilinear model of the ADAS devices was used for calculating the inelastic response of the test structure.

Following these studies, questions concerning the general implementation of ADAS elements remained. For example, for purposes of general design, how do the ADAS device parameters affect the inelastic response of building structures, and how can these parameters be properly selected taking into consideration the earthquake ground-motion characteristics, intensity, and energy content. Answers to these questions was the motivation for the research presented in this paper.

The objective of this research was to study the influence of ADAS element parameters on the inelastic response of some building structures. These results provide a better understanding of the ADAS parameters and their effects on building seismic response and can be used as a source document for the design of building structures with ADAS elements.

ANALYTICAL MODELING OF ADAS ELEMENTS

A bilinear model was selected to represent the ADAS device inelastic behavior because of its mathematical simplicity and its ability to account for both strain hardening and hysteretic behavior. The hysteretic energy dissipated by the device in a loading cycle, as shown in Fig. 3, is a function of the yield force, P_y , the yield displacement, Δ_y , and the ductility ratio, $\mu = (\Delta/\Delta_y)$

$$W_b = 4P_y\Delta_y(\mu - 1) \dots\dots\dots (1)$$

This hysteretic energy is independent of the strain-hardening ratio that determines the force increase due to material hardening.

The selected parameters of ADAS elements included: (1) The yield force and the yield displacement of ADAS devices; (2) the ratio of the horizontal bracing member stiffness to the ADAS device initial elastic stiffness, B/D

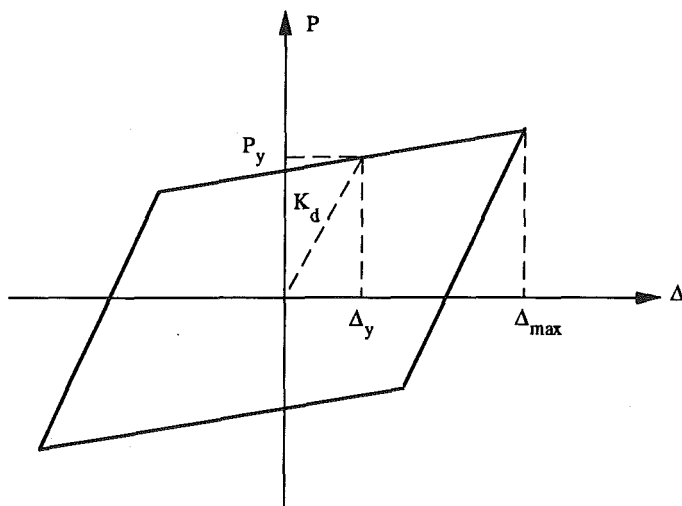


FIG. 3. Bilinear Model for ADAS Device

ratio; (3) the ratio of the ADAS element stiffness to the structural story stiffness without ADAS elements in place, SR ratio; and (4) the device strain-hardening ratio.

As illustrated in Fig. 1, an ADAS element will be defined as an ADAS device and two bracing members that support the device. The horizontal stiffness of the ADAS element, K_a , is a function of the lateral stiffness of the bracing members, K_b , and the device initial stiffness, $K_d = P_y/\Delta_y$. That is

$$K_a = \frac{K_b K_d}{K_b + K_d} \dots \dots \dots (2a)$$

or

$$K_a = \frac{K_d}{1 + \frac{1}{\left(\frac{B}{D}\right)}} \dots \dots \dots (2b)$$

where $B/D = K_b/K_d$. The SR ratio is defined as the ratio of the horizontal ADAS element stiffness to the structural story stiffness without ADAS elements in place, K_s .

$$SR = \frac{K_a}{K_s} \dots \dots \dots (3)$$

The interrelationship of ADAS device parameters can be expressed as follows:

$$P_y = SR \cdot K_s \left[1 + \frac{1}{\left(\frac{B}{D}\right)} \right] \Delta_y \dots \dots \dots (4)$$

The frames used in this study are a 10-story cross-braced moment frame (Workman 1969), identified by WMAN, and a 10-story moment frame (Akkari 1984), with properties as given in Tables 1 and 2. In this study, two Akkari cases were considered: the frame with a concentrated weight at the roof that is three times the weight of other floors, identified by AKKCM, and the frame with uniform weight distribution, identified by AKKUM. The original Workman frame was designed as a core-braced frame providing lateral support to three bays of frames. Thus, the girder span is short, but the floor weights are normal.

The minimum design base shear forces for these frames are calculated

TABLE 1. 10-Story Workman and Akkari Frame Properties

(1)	Workman frame (2)	Akkari frame (3)
Story height	all at 144 in.	first at 180 in.; all other at 144 in.
Floor weights	all at 132 kips	all at 79.13 kips; AKKCM roof 260.53 kips
Girder span	single at 240 in.	single at 360 in.

TABLE 2. 10-Story Workman and Akkari Frame Properties

Floor level (1)	Workman Frame			Akkari Frame	
	Girder I in. ⁴ (2)	Column I in. ⁴ (3)	Bracing A sq. in. (4)	Girder I in. ⁴ (5)	Column I in. ⁴ (6)
10	800.6	—	—	515.5	—
9	800.6	339.2	2.88	800.6	796.8
8	800.6	542.1	2.88	800.6	796.8
7	800.6	542.1	2.88	1,326.8	796.8
6	800.6	851.2	2.88	1,326.8	1,266.5
5	984.0	851.2	2.88	1,326.8	1,266.5
4	984.0	1,165.8	2.88	1,478.3	1,266.5
3	984.0	1,165.8	2.94	1,478.3	1,786.8
2	984.0	1,373.1	2.94	1,478.3	1,786.8
1	1,286.8	1,373.1	3.38	1,814.5	1,786.8
—	—	2,274.8	0	—	2,149.6

TABLE 3. Minimum Design Base Shear Forces ($R_w = 12$)

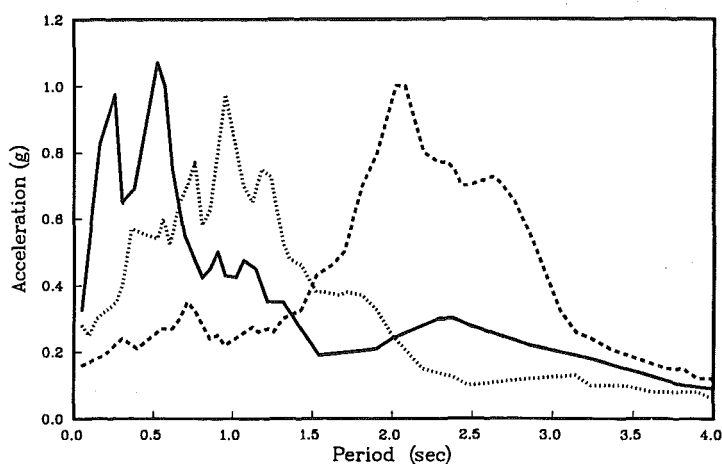
Frame (1)	Z (2)	I (3)	C/R_w minimum (4)	ZIC/R_w minimum (5)	W kips (6)	$V_b = ZICW/R_w$ kips (7)
WMAM	0.4	1.0	0.075	0.03	1,320.0	39.6
AKKUM	0.4	1.0	0.075	0.03	791.3	23.7
AKKCM	0.4	1.0	0.075	0.03	972.7	29.2

according to the *Uniform Building Code* (1988). As shown in Table 3, the minimum value of $C/R_w = 0.075$ is used to determine the minimum design base shear, which is 3% of the building weight in seismic zone 4. Many designers will consider this to be an extremely low base shear coefficient for a 10-story building. It must be remembered that the moment frame system will be designed for the expected earthquake design forces as if the ADAS bracing is not in place; therefore, the stiffness of the system will be much lower than for the complete system. Drift limits of the *Uniform Building Code* (1988) will apply to the moment frames only with the ADAS bracing in place. The period T_1 associated with this minimum design base shear value is 1.64 s, when calculated from $C_{min} = 0.075R_w = 1.25 S/T_1^{2/3}$ for a soil factor, $S = 1$. The periods for the unbraced frames for all cases is much larger than 1.64 s so the C_{min} value of 0.90 is used. The periods of the frames with ADAS and bracing for different SR ratios, the design base shear forces, and the ADAS device yield forces in terms of the design story shear forces are summarized in Table 4. The values in Table 4 are based on the calculated K_e values of these frames and the conditions of $B/D = 2$ and $\Delta_y = 0.2$ in. Device yield forces for other B/D ratios or device yield displacements can be calculated using (4) and the values given in this table.

The earthquake ground-acceleration records used in this study were selected to cover a broad range of building periods. The selected records include the 1940 El Centro (NS component), the 1985 Mexico (SCT Station, EW component), and the 1978 Miyagi-Ken-Oki. The response spectral accelerations of these three normalized earthquake records are shown in Fig. 4. By comparing the elastic periods of these buildings for different SR values

TABLE 4. Design Base Shear and ADAS Yield Force of Frames with Different SR Ratios ($B/D = 2$; $\Delta_y = 0.2$ in.; $V_{bmin} = 3\% W$)

SR (1)	WMAN			AKKUM			AKKCM		
	T sec (2)	V_b kips (3)	$P_y = V_s$ (4)	T sec (5)	V_b kips (6)	P_y/V_s (7)	T sec (8)	V_b kips (9)	P_y/V_s (10)
1	2.32	39.6	1.3	1.78	23.7	1.9	2.25	28.7	1.5
2	1.89	39.6	2.4	1.45	25.8	3.3	1.84	28.7	2.9
3	1.64	39.6	3.2	1.26	28.3	4.6	1.60	29.7	3.7
4	1.47	42.6	4.0	1.13	30.4	5.8	1.43	32.0	4.6
5	1.34	45.3	4.7	1.03	32.4	6.8	1.30	34.1	5.4
6	1.24	47.7	5.4	0.95	34.1	7.8	1.21	35.7	6.2
7	1.16	49.9	6.1	0.89	35.7	8.7	1.12	37.4	6.9
8	1.09	52.0	6.7	0.84	37.1	9.6	1.06	39.0	7.6
9	1.04	53.6	7.3	0.80	38.8	10.5	1.01	40.3	8.3
10	0.99	55.4	7.9	0.76	39.6	11.3	0.96	41.7	8.9



1940 El Centro Earthquake

1978 Miyagi-Ken-Oki Earthquake

1985 Mexico Earthquake

FIG. 4. Elastic Acceleration Response Spectra for Three Earthquakes

(Table 4) with the elastic response spectra in Fig. 4, it can be estimated that the El Centro record will result in small responses because its peak acceleration spectra occurs at less than 1 sec. The Miyagi-Ken-Oki record will have the greatest effect on the buildings with periods of about 1 s, and the Mexico record will have the greatest effect on buildings with periods of 1.6–2.6 s. Earthquake record scale factors (ERSF) were used to evaluate the effect of different earthquake intensities. The maximum earthquake ground accelerations for the selected ERSF are given in Table 5.

TABLE 5. ERSF and Maximum Earthquake Ground Accelerations

Earthquake (1)	ERSF ^a (2)	Maximum acceleration (3)
El Centro 1940	1.0	0.31g
El Centro 1940	2.0	0.63g
Mexico 1985	1.0	0.17g
Mexico 1985	1.5	0.26g
Miyagi-Ken-Oki 1978	1.0	0.26g
Miyagi-Ken-Oki 1978	2.0	0.53g

^aERSF = earthquake record scale factor.

The DRAIN-2D (Kanaan and Powell 1973) program was modified to analyze the frames with ADAS elements by adding a subroutine to model the hysteretic behavior of ADAS devices. Energy options that calculate the total absolute input energy (Uang and Bertero 1988), E_i , the elastic vibration energy, E_e , the energy dissipated by inherent viscous damping, E_d , the hysteretic energy dissipated by the ADAS devices, E_{adas} , and the hysteretic energy absorbed by other structural members, E_m , were added to the program. In this study, the elastic vibration energy is defined as the sum of the kinetic energy and the elastic strain energy. The energy balance in a building structure can be expressed as follows:

$$E_i = E_e + E_d + E_{adas} + E_m \dots \dots \dots (5)$$

RESPONSE OF FRAMES WITH ADAS ELEMENTS

The selected response parameters include: (1) The story displacement, which is the relative drift between two stories; (2) the story shear force; (3) the ADAS device shear force; and (4) the ADAS device ductility ratio.

Effect of ADAS Device Strain-Hardening Ratio

To study the effect of ADAS device strain-hardening ratio on the inelastic response of a building structure, hardening ratios of 1%, 4%, 8%, and 10% were used in the calculation of the responses of the AKKUM frame subjected to the El Centro earthquake, which are shown in Figs. 5(a–h). It can be seen from these figures that the strain-hardening ratio has little influence on the inelastic displacement response and device ductility ratios, Figs. 5(a–d), for this building frame and selected earthquake. But the ADAS forces and story shear forces increased as the hardening ratios increased, Figs. 5(e–h). The effect of hardening ratio was more significant for a stronger earthquake (ERSF = 2), which generated larger ADAS ductilities. For design purposes, the hysteretic behavior and the energy dissipation capacity of an ADAS device can be based on the yield force P_y , but for design of the bracing members supporting the ADAS device, the effect of strain hardening should be taken into account.

Effect of B/D Ratios

The effect of B/D ratio on reducing the structural inelastic response was studied by calculating the responses of the AKKUM frame with different B/D ratios. The story displacement and the ADAS device ductility ratio responses, Figs. 6(a–b), illustrate two cases from a study of the conse-

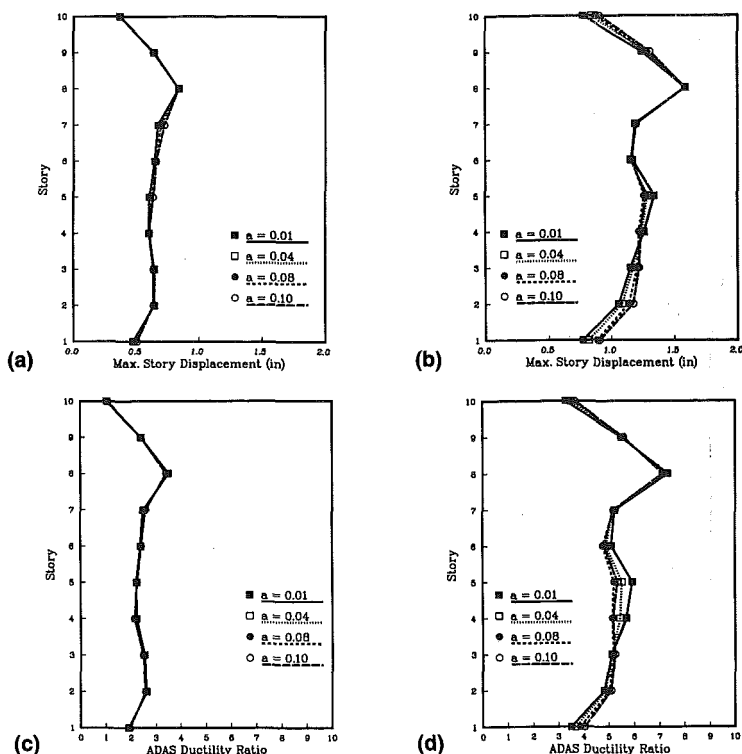


FIG. 5. (a) Story Displacement Response of AKKUM Frame with ADAS Elements Subjected to El Centro Earthquake, ERSF = 1.0; SR = 2.0; (b) Story Displacement Response of AKKUM Frame with ADAS Elements Subjected to El Centro Earthquake, ERSF = 2.0; SR = 2.0; (c) ADAS Ductility Ratios of AKKUM Frame with ADAS Elements Subjected to El Centro Earthquake, ERSF = 1.0; SR = 2.0; and (d) ADAS Ductility Ratios of AKKUM Frame with ADAS Elements Subjected to El Centro Earthquake, ERSF = 2.0; SR = 2.0

quences of different B/D ratios by Xia et al. (1990). The results show that B/D ratios had little influence on the inelastic response except some minor increase in the displacement response for B/D ratios smaller than 2.

The B/D ratio will effect the deformation of the ADAS devices only before they yield. After yielding, the stiffness of ADAS device decreases significantly due to inelastic deformations within the device regardless of the stiffness of the bracing members. It would be uneconomical to try to improve seismic response of structures by using large B/D ratios. Considering the cost of bracing members, it is recommended that a B/D ratio of about 2 be used for the design of the ADAS elements unless the brace strength necessary to yield the ADAS device without buckling in compression or yielding in tension results in a larger B/D ratio.

Effect of Device Yield Displacement, Device Yield Force, and SR Ratio

Among the three parameters of Δ_y , P_y , and SR , only two are independent, and the other can be determined from (4). In this study, the device yield

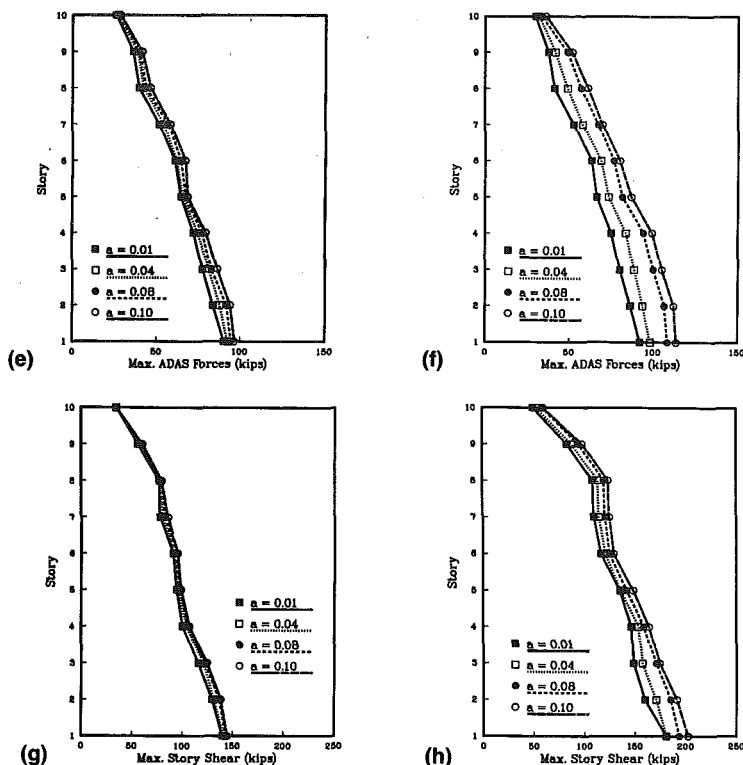


FIG. 5. (e) ADAS Force Response of AKKUM Frame with ADAS Elements Subjected to El Centro Earthquake, ERSF = 1.0; SR = 2.0; (f) ADAS Force Response of AKKUM Frame with ADAS Elements Subjected to El Centro Earthquake, ERSF = 2.0; SR = 2.0; (g) Story Shear Response of AKKUM Frame with ADAS Elements Subjected to El Centro Earthquake, ERSF = 1.0; SR = 2.0; and (h) Story Shear Response of AKKUM Frame with ADAS Elements Subjected to El Centro Earthquake, ERSF = 2.0; SR = 2.0

displacement and SR ratio were chosen to be explicit variables, and the device yield force was determined from (4). To study the effect of these parameters on the inelastic response of building frames, WMAN, AKKUM, and AKKCM frames were analyzed using different combinations of SR ratio and yield displacement.

The results show that the ADAS ductility ratio is very sensitive to the device yield displacement. This device yield displacement is more effective than the SR ratio or the device yield force in controlling the maximum device ductility ratio. As an example, the response of AKKUM frame subjected to the El Centro earthquake is used. It can be seen from Fig. 7(a) that device yield displacement has minor influence on the story displacement response. But its influence on the device ductility ratio is significant when it is small, as shown in Fig. 7(b). To optimize the device energy dissipation effectiveness, it is desirable to have a small device yield displacement. However, the device yield displacement should be large enough to limit excessive device ductility for severe earthquake ground motions. A device yield dis-

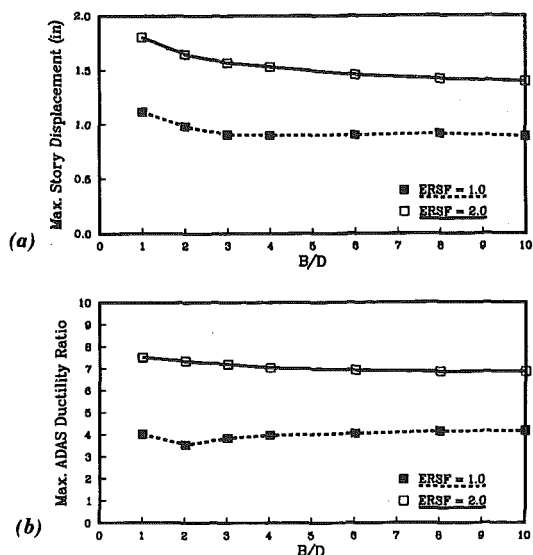


FIG. 6. (a) Maximum Story Displacements of AKKUM Frame for Different B/D Ratios, El Centro Earthquake; $SR = 2.0$; $\Delta_y = 0.2$ in.; and (b) Maximum ADAS Ductility Ratios of AKKUM Frame for Different B/D Ratios, El Centro Earthquake; $SR = 2.0$; $\Delta_y = 0.2$ in.

placement between 0.2 in. and 0.3 in. (0.0014H and 0.002H) with a target device ductility of 4–5 results in a maximum story drift of about 0.6–1.0%.

The influence of SR on the displacement response can be observed in Figs. 8(a and b). The results show that the displacement response decreases with increase in SR ratios, but the effectiveness of increasing the SR ratio is not linear. It is relatively ineffective at larger SR ratios and varies depending on the characteristics of the earthquake. The effect of the selected SR value is significant when SR is less than 2 for the El Centro earthquake and when SR is less than 4 for the Mexico earthquake. The effect of SR on reducing inelastic response is insignificant for SR ratios higher than these values. In Figs. 8(a and b), the device yield displacement was held constant. From (4), it can be seen that for this condition, the device yield force increases with increases in SR ratio. In other words, the effect of increasing yield force is similar to the effect of increasing SR ratios. That is, increasing device yield force can effectively reduce the inelastic response of a building structure within a certain range. The device yield force needed to control inelastic displacement depends on the expected earthquake intensity, ground-motion characteristics, and energy demands. Therefore, the SR ratio should be selected to satisfy both building stiffness requirements and the effect of SR ratio in reducing inelastic response.

Increasing the ADAS device yield force will increase the device strength and the hysteretic energy dissipation capacity for equal displacements. From the point of view of strength and energy dissipation, it is desirable to select a large ADAS yield force. However, a large yield force will increase the size of the supporting structural members and the cost of the devices. The proper selection of the ADAS yield force should consider both structural safety and cost. Based on the response of these structures subjected to the

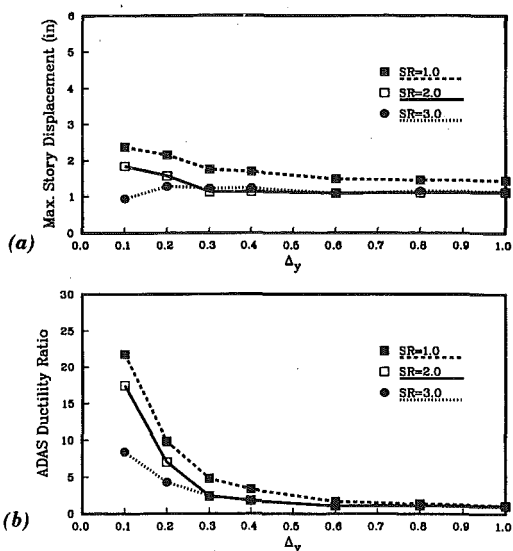


FIG. 7. (a) Maximum Story Displacements of AKKCM Frame for Different Yield Displacements, El Centro Earthquake, ERSF = 1.0; $B/D = 2.0$; and (b) Maximum ADAS Ductility Ratios of AKKCM Frame for Different Yield Displacements, El Centro Earthquake, ERSF = 1.0; $B/D = 2.0$

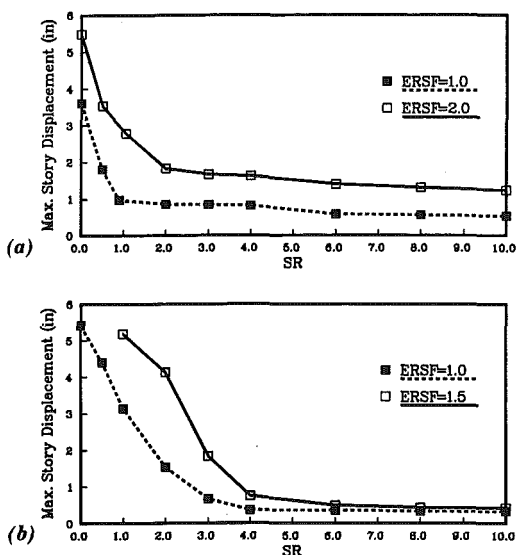


FIG. 8. (a) Maximum Story Displacements of AKKUM Frame for Different SR Ratios, El Centro Earthquake, $\Delta_y = 0.2$ in.; and (b) Maximum Story Displacements of AKKUM Frame for Different SR Ratios, Mexico Earthquake, $\Delta_y = 0.2$ in.

El Centro earthquake, which has a response spectra similar to the *Uniform Building Code* (1988) seismic design spectra, an SR ratio about 2 was appropriate for the design of ADAS devices and bracing members. From Table 4, it can be seen that the average device yield force for the three frames with $SR = 2$ is about three times the minimum design shear force. The device yield force at the base for $SR = 2$ is about 9% of the building seismic weight, which corresponds to about 5% on a working stress basis. It should be remembered that the minimum design base shear force of 3% of the building weight was the consequence of using the moment frame properties without consideration of drift limits. The ADAS and bracing provide deflection control for the building.

Energy Response

The energy response of the frames with and without ADAS elements was calculated to show the effectiveness of ADAS device energy dissipation. The results show that for frames without ADAS elements, subjected to a strong earthquake, the hysteretic energy dissipated by structural members E_m , was very large. E_m was about 50%–80% of total input energy depending on the earthquake characteristics and the intensity. As an example, the energy response of WMAN frame without ADAS elements, subjected to the Mexico earthquake, is shown in Fig. 9(a), in which the hysteretic energy dissipated by structural members is very high (about 8,000 k-in. or about 80% of the total input energy). As a comparison, the energy response of the WMAN frame with ADAS elements ($SR = 3$; and $\Delta_y = 0.3$) is shown in Fig. 9(b), which indicates that ADAS elements dissipated a large amount of hysteretic energy (the distribution throughout the height of the building is given in Table 6) and substantially reduced the hysteretic energy dissi-

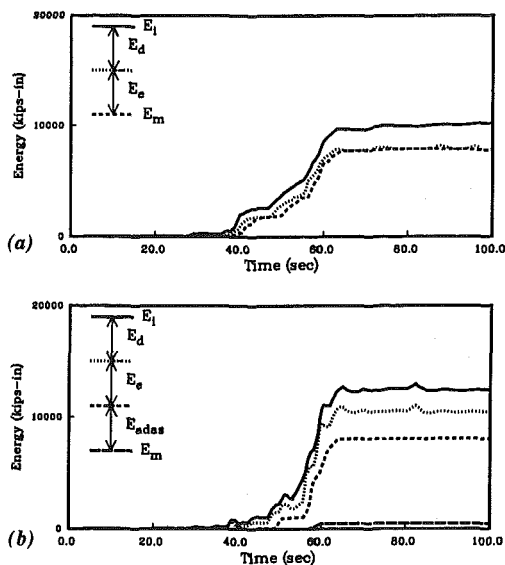


FIG. 9. (a) Energy Histories for WMAN Moment Frame Subjected to Mexico Earthquake, ERSF = 1.0; and (b) Energy Histories for WMAN Frame with ADAS Elements Subjected to Mexico Earthquake, ERSF = 1.0; $SR = 3.0$; $\Delta_y = 0.3$ in.; $B/D = 2.0$

TABLE 6. ADAS Device Energy Response of WMAN Frame with $SR = 3.0$; $B/D = 2$; and $\Delta_y = 0.3$ in. (kips-in.)

Story (1)	El Centro		Miyagi-Ken-Oki		Mexico	
	ERSF = 1.0 (2)	ERSF = 2.0 (3)	ERSF = 1.0 (4)	ERSF = 2.0 (5)	ERSF = 1.0 (6)	ERSF = 2.0 (7)
10	0.0	47.2	0.0	21.4	0.0	2.2
9	48.7	291.4	4.3	270.4	0.0	5.9
8	122.5	581.1	327.4	1,565.7	527.8	1,016.1
7	51.8	445.0	540.4	2,036.7	913.5	1,894.9
6	35.3	485.4	552.9	1,797.9	1,494.2	2,989.2
5	16.3	451.6	343.6	1,215.4	1,513.2	2,949.3
4	56.3	619.5	486.1	1,106.5	1,941.9	3,364.7
3	74.7	817.6	224.3	1,022.4	2,425.7	5,015.4
2	46.5	831.0	394.4	1,728.9	5,904.3	12,131.0
1	2.1	163.7	161.2	439.0	467.2	797.9

Note: ERSF = earthquake record scale factor.

pation demands on structural members, E_m , to nearly zero in this case. From Table 4, it can be seen that the WMAN frame with $SR = 3$ has an elastic period of 1.64 sec. The Mexico City spectra, Fig. 4, shows that as the ADAS devices yield (the effective period of the frame increases), the maximum response should increase. In this case, the maximum story displacement of about 3 in. occurred at the third level. With $\Delta_y = 0.3$ in., the maximum ADAS ductility was less than 10. It can be seen that the ADAS elements yield first at smaller displacements, and the structural members yield second at larger displacements. Thus, the structural member inelastic capabilities will not come into play until severe earthquake responses occur.

The results also show that the energy demands on the ADAS devices vary depending on the earthquake characteristics and intensity. The ADAS-device energy dissipation for WMAN frame is listed in Table 6. It can be seen that the ADAS-device energy requirements for the Mexico earthquake are significantly higher than the energy requirements for the Miyagi-Ken-Oki earthquake or the El Centro earthquake. It seems possible to design the ADAS devices according to the device energy dissipation capacity and the seismic energy demands of an earthquake, if the earthquake energy demand can be quantified by its expected ground-motion intensity and duration. No attempt was made to do this in this research effort.

CONCLUSIONS

Properly designed ADAS elements can be used to effectively control the inelastic response of a building frame. In the design of frames with ADAS elements, it is important to select appropriate values of the ADAS-device parameters such as the device yield force, the device yield displacement, and the stiffness ratio of the ADAS element stiffness to the frame story stiffness, SR . Based on the limited analytical results from three structural systems and three earthquake records used in this study, the following conclusions are presented.

ADAS elements can significantly increase the structural energy dissipation capacity and substantially reduce the energy dissipation demands on

other frame members. As a result of the increased energy dissipation capacity at small displacements, structural safety is increased.

The selection of device yield force should consider both strength and energy demands based on the expected earthquake ground-motion intensity and duration at the building site. The yield force should be large enough to provide adequate energy dissipation capacity within the desired design ductility ratio. For a selected yield force and yield displacement, the elastic stiffness of the ADAS device and the stiffness ratio SR can be calculated.

ADAS ductility ratio is sensitive to the device yield displacement. To avoid device ductility ratios beyond $\Delta_y = 10$, proper selection of device yield displacement is very important. From the studies discussed in this paper, the recommended device yield displacement for design of the ADAS elements is in the range of $0.0014H$ – $0.002H$.

The effect of brace stiffness to device stiffness ratio, B/D , on reducing structural inelastic response is small. A B/D value equal to 2 is recommended for bracing member design, provided that the bracing has enough strength to yield the ADAS devices. The effect of strain hardening on ADAS device forces should be taken into consideration for design of the bracing members and other structural members supporting ADAS devices.

The energy dissipation capacity of an ADAS device can be based on the yield force, P_y , and yield displacement, Δ_y , as given in (1).

As part of this research, a design procedure and criteria for the design of buildings with ADAS elements was proposed based on the analytical study of ADAS device parameters described herein. The design procedure and criteria illustrated by a design example will be published in a separate paper.

ACKNOWLEDGMENTS

This paper is part of the study of building frames with supplemental and mechanical damping elements that was sponsored by the National Science Foundation (NSF) through Grant numbers CES-8821735 and BCS-9114755. The authors extend their appreciation to NSF for their financial support. The views and opinions expressed in this paper are those of the authors and do not necessarily represent the views of NSF.

APPENDIX I. CONVERSION TO SI UNITS

<u>To convert</u>	<u>To</u>	<u>Multiply by</u>
in.	m	0.0254
in./sec	m/s	0.0254
in./sec ²	m/s ²	0.0254
kip	kN	4.448N

APPENDIX II. REFERENCES

- Akkari, M. M. (1984). "Nonlinear dynamic analysis using mode superposition," PhD thesis, University of California, Davis, Calif.
- Bergman, D. M., and Hanson, R. D. (1986). "Characteristics of viscoelastic mechanical damping devices." *Proc., ATC Seminar on Base Isolation and Passive Energy Dissipation*, Applied Technology Council, Redwood City, Calif.
- Bergman, D. M., and Hanson, R. D. (1990). "Viscoelastic versus steel plate mechanical damping devices: An experimental comparison." *Proc., 4th U.S. Nat.*

- Conf. on Earthquake Engrg.*, Earthquake Engineering Research Institute, Oakland, Calif.
- Hanson, R. D. (1986). "Basic concepts and potential applications of supplemental mechanical damping for improving earthquake resistance." *Proc., ATC Seminar on Base Isolation and Passive Energy Dissipation*, Applied Technology Council, Redwood City, Calif.
- Kanaan, A. E., and Powell, G. H. (1973). "General purpose computer program for inelastic dynamic response of plane structures." *Report No. UCB/EERC-73/6*, Univ. of California at Berkeley, Berkeley, Calif.
- Scholl, R. E. (1990). "Improve the earthquake performance of structures with added damping and stiffness elements." *Proc., 4th U.S. Nat. Conf. on Earthquake Engrg.*, Earthquake Engineering Research Institute, Oakland, Calif.
- Steimer, S. F., and Chow, F. L. (1984). "Curved plate energy absorbers for earthquake resistant structures." *Proc., 8th World Conf. on Earthquake Engrg.*, Earthquake Engineering Research Institute, Oakland, Calif., Vol. V, 967-974.
- Su, Y.-F., and Hanson, R. D. (1990a). "Comparison of effective supplemental damping: Equivalent viscous and hysteretic." *Proc., 4th Nat. Conf. on Earthquake Engrg.*, Earthquake Engineering Research Institute, Oakland, Calif.
- Su, Y.-F., and Hanson, R. D. (1990b). "Seismic response of building structures with mechanical damping devices." *Report UMCE 90-2*, Univ. of Michigan, Ann Arbor, Mich.
- Uang, C. M., and Bertero, V. V. (1988). "Use of energy as a design criterion in earthquake resistant design." *Report No. EERC 88-18*, Earthquake Engr. Res. Ctr., Univ. of California at Berkeley, Berkeley, Calif.
- Uniform building code.* (1988). Int. Conf. of Bldg. Officials, Whittier, Calif.
- Whittaker, A. S. Bertero, V. V., Alonso, L. J., and Thompson, C. (1989). "Earthquake simulator testing of steel plate added damping and stiffness elements." *Report No. UCB/EERC-89/02*, Earthquake Engr. Res. Ctr., Univ. of California at Berkeley, Berkeley, Calif.
- Workman, G. H. (1969). "The inelastic behavior of multistory braced frame structures subjected to earthquake excitation," PhD thesis, Univ. of Michigan, Ann Arbor, Mich.
- Xia, C., Hanson, R. D., and Wight, J. K. (1990). "A study of ADAS element parameters and their influence on earthquake response of building structures." *Report UMCE 90-12*, Univ. of Michigan, Ann Arbor, Mich.

APPENDIX III. NOTATION

The following symbols are used in this paper:

- $B/D = K_b/K_d$, ratio of bracing member stiffness to device elastic stiffness;
 $C = 1.25S/T_1^{2/3}$, numerical coefficient used in *Uniform Building Code* (1988) to determine base shear;
 $C_{\min} = 0.075 R_w$, minimum value of C ;
 E_{adas} = hysteretic energy dissipated by ADAS devices;
 E_d = energy dissipated by inherent viscous damping;
 E_e = elastic vibration energy, which is sum of kinetic energy and elastic strain energy;
 E_i = total absolute input energy;
 E_m = hysteretic energy absorbed by other structural members;
 H = story height;
 I = structural importance factor;
 $K_a = (K_b K_d)/(K_b + K_d)$, horizontal stiffness of ADAS element;
 K_b = stiffness of bracing members;
 $K_d = P_y/\Delta_y$, device elastic stiffness;
 K_s = structural story stiffness;

- P_y = ADAS device yield force;
 R_w = 12, numerical coefficient used in *Uniform Building Code* (1988) to determine base shear;
 S = site coefficient for soil characteristics;
 SR = K_a/K_s , ratio of horizontal ADAS element stiffness to structural story stiffness;
 T = structural period;
 T_1 = $(1.25S/C_{min})^{3/2}$, structural period associated with C_{min} ;
 V_b = structural base shear force;
 V_s = structural story shear force;
 W = structural weight;
 W_b = hysteretic energy dissipated by device in loading cycle;
 Z = seismic zone factor;
 Δ_y = ADAS device yield displacement; and
 μ = the ADAS device ductility ratio.